


# Effect of particle surface treatment and blending method on flexural properties of injection-molded cenosphere/HDPE syntactic foams

B. R. Bharath Kumar<sup>1</sup> · Mrityunjay Doddamani<sup>1</sup> · Steven E. Zeltmann<sup>2</sup> ·  
Nikhil Gupta<sup>2</sup>  · Uzma<sup>3</sup> · S. Gurupadu<sup>3</sup> · R. R. N. Sailaja<sup>3</sup>

Received: 1 September 2015 / Accepted: 21 December 2015 / Published online: 4 January 2016  
© Springer Science+Business Media New York 2015

**Abstract** The present work on cenosphere/high-density polyethylene (HDPE) syntactic foams aims at understanding the effect of surface treatment of cenospheres and functionalization of HDPE on flexural properties. Cenospheres are treated with silane, and HDPE is functionalized with 10 % dibutyl maleate. Effects of mechanical and Brabender mixing methods are also studied. Flexural test specimens are cast with 20, 40, and 60 wt% of cenospheres using injection molding. The flexural modulus and strength are found to increase with increasing cenosphere content. Particle breakage increases with the cenosphere content, and the measured properties show increased dependence on processing method. Brabender mixing resulted in 70 and 41 % higher modulus and strength for 60 wt% cenospheres than HDPE. Modulus of syntactic foams is predicted by two theoretical models. Bardella–Genna model provides close estimates for syntactic foams having 20 and 40 wt% cenospheres, while predictions are higher for higher cenosphere content, likely due to particle breakage during processing. The uncertainty in the properties of

cenospheres due to defects contributes to the variation in the predicted values.

## Introduction

Hollow particle-filled composites called syntactic foams are lightweight materials that are used in structural applications due to their excellent specific compressive strength and stiffness [1]. The existing applications of these materials include underwater vehicle structures, submarine buoyancy modules, buoys, aircraft parts, and thermoforming plugs [2]. Most of the existing studies on syntactic foams are available on epoxy and vinyl ester matrices. In comparison, studies on thermoplastic matrix syntactic foams are scarce as summarized in chapters of a recent book [3, 4]. Low- and high-density polyethylene (LDPE and HDPE), polymethyl methacrylate, and polylactic acid [5, 6] are among the thermoplastic resins that are widely used in fabricating consumer products. Use of these resins in fabricating syntactic foams can provide opportunities of saving weight in existing applications and also in developing new applications. One of the advantages of using thermoplastic resins is the possibility of using rapid manufacturing industrial techniques for making syntactic foam parts. Therefore, it is of great interest to develop and study thermoplastic resin syntactic foams.

Hollow glass particles and cenospheres have been used as fillers in syntactic foams. Fly ash, an industrial waste material generated in coal fired power plants, contains hollow particles called cenospheres [7, 8]. Alumina and silica are the main constituents of cenospheres, which have higher mechanical properties than glass [9]. Use of such industrial waste material can help in addressing the fly ash disposal and also in creating high-performance syntactic

---

✉ Nikhil Gupta  
ngupta@nyu.edu

Mrityunjay Doddamani  
mrdoddamani@nitk.edu.in

<sup>1</sup> Lightweight Materials Laboratory, Department of Mechanical Engineering, National Institute of Technology Karnataka, Surathkal, India

<sup>2</sup> Composite Materials and Mechanics Laboratory, Mechanical and Aerospace Engineering Department, Tandon School of Engineering, New York University, Brooklyn, NY 11201, USA

<sup>3</sup> The Energy and Resources Institute (TERI), Southern Regional Center, Bangalore 560 071, India

foams [10–12]. Cenosphere-reinforced thermoset composites are widely investigated in the literature for structural applications [13–16]. The present work uses fly ash cenospheres for developing syntactic foams. These particles have numerous defects present in their walls and are not perfectly spherical, which compromises their properties compared to engineered particles with perfect walls and spherical shape. The alumino-silicate composition of cenospheres compensates for the loss in mechanical properties due to the presence of defects, and their properties are generally in the range observed for the commonly used glass microballoons [16].

Polyolefins like HDPE are non-polar and hydrophobic and do not show compatibility with glass particles and cenospheres, which results in cluster formation and poor interfacial bonding. Hence, functionalization of HDPE and surface modification of cenospheres are desirable to promote bonding between them. The adhesion-promoting ability of coupling agents produces a molecular bridge between the inorganic filler and the organic matrix that results in covalent bonds, contributing toward improved adhesion. Earlier work carried out by the authors using a combination of hollow glass particles and cenospheres exhibited enhanced mechanical properties of syntactic foams due to improved interfacial bonding through functionalization of particles and resin [17]. Cenospheres were treated with silane to improve the interfacial bonding in different matrix resins [18, 19]. Other available studies on silane-treated cenosphere-filled polyethylene matrix syntactic foams have restricted cenosphere concentration to 20 wt% [20]. At such low concentration, the particle-to-particle interaction effects are negligible. Both tensile strength and elongation to break reduced as the cenosphere concentration was increased in the syntactic foam. Dielectric properties of these composites are also found studied [21]. Functionalized HDPE has been used with untreated glass hollow particle fillers [22, 23]. Functionalization of polymer for compatibility with different reinforcing elements is described in previous studies [17, 24–27]. Chiu et al. [28] observed that maleic anhydride-functionalized polyolefins led to improved impact strength in polypropylene/polyethylene blend. Work on amino ester-functionalized HDPE shows that apart from the matrix functionalization, it is necessary to modify the surface of inorganic fillers to promote interfacial bonding [29]. Improved impact strength owing to surface modification of cenospheres has been observed by Gu et al. [30]. Enhanced photocatalytic activity has been found by modifying cenospheres with  $\text{TiO}_2$  [31]. Silane-treated cenospheres led to improved dispersion in cenosphere filled ABS composites as reported by Desai et al. [32]. This treatment resulted in an increase in the tensile modulus and strength of syntactic foams but the fracture toughness remained unaffected compared to the corresponding compositions that did not contain matrix functionalization.

Another study used polypropylene as the matrix resin with cenosphere fillers [33]. In the absence of strong interfacial bonding, due to lack of surface treatment of cenospheres, the study showed gain in flexural modulus (about 27 %) but the flexural strength was reduced (about 8 %) as the cenosphere content was increased to 20 wt%.

Recent studies on syntactic foams investigated their three-point bending characteristics in either flexural [34–37] or short-beam shear test configurations [38–40]. It is observed that the dependence of flexural modulus on the microballoon wall thickness and volume fraction is often complex. The stiffening effect of such low-density hollow particles is dependent on the relative modulus of the particle material and matrix resin as well as particle wall thickness. Most of the available studies have used engineered glass microballoons made of soda-lime-borosilicate glass as the filler material [41, 42]. Environmental exposure of such syntactic foams has shown that dealcalization of glass can lead to severe particle and syntactic foam degradation [43]. Cenospheres may be advantageous in such situations due to their alumino-silicate composition.

Several challenges can be identified related to thermoplastic syntactic foams based on the existing observations. While use of high volume fraction of hollow particles can provide lower density syntactic foams, most of the current literature has studied thermoplastic syntactic foams with up to 20 wt% particles. The available studies on thermoplastic syntactic foams process materials under controlled conditions at laboratory scale, which usually provides syntactic foams with high quality. However, processing of materials with industrial-scale manufacturing equipment may not yield similar quality so the effect of such manufacturing environment needs to be studied, which is the focus of the present work. Rapid manufacturing is a key to satisfying the ever growing demands of useful and durable products. The present work deals with utilization of one such technique, injection molding, with optimized temperature and pressure to synthesize syntactic foams. Cenospheres were surface treated with silane coupling agent, and dibutyl maleate was used for HDPE functionalization to promote interfacial bonding. Amine groups on the silane-treated cenospheres bond efficiently with the ester groups of DBM. The possible reaction scheme between silane-treated cenosphere and functional groups of HDPE is presented in Fig. 5 of [17]. The fabricated specimens are characterized for flexural properties.

## Experimental

### Materials

The matrix material is chosen as HDPE of grade HD50MA180 (melt flow index of 20 g/10 min) supplied

by Reliance Polymers, Mumbai, India. The resin is in the form of pellets with molecular weight between  $2 \times 10^5$  and  $3 \times 10^6$ . Cenosphere of CIL-150 grade, supplied by Cenosphere India Pvt. Ltd., Kolkata, India, is used as hollow fillers. 3-Amino propyl tri ethoxy silane (APTS) was procured from Sigma Aldrich (USA). Dibutyl maleate (DBM) and dicumyl peroxide were procured from S.D. Fine-Chem Ltd., Mumbai, India.

Chemical, physical, and sieve analysis results provided by the supplier of cenospheres are presented in Table 1. Cenospheres primarily comprise alumina, silica, calcium oxide, and iron oxides. Particle size and shape analysis is conducted using a Sympatec (Pennington, NJ) QICPIC high-speed image analysis system. The particles are dispersed using the RODOS and VIBRI systems, which aerosolize a stream of particles in a jet of compressed air. A pulsed laser illuminates the particles as they pass a camera that images the particles at 175 frames/s. For each particle imaged, the equivalent diameter is calculated as the diameter of a sphere having a projected area equal to the projection captured by the camera. Two runs of each particle type are conducted, and the values presented are averaged from these runs, with weight according to the number of particles in each run. Approximately, 375,000 and 550,000 particles are measured for untreated and treated particles, respectively.

*Silane treatment of cenospheres*

The silane treatment of cenospheres has been described in earlier work [17, 44]. A mixture of water/ethanol (20:80 wt%) was prepared and maintained at 80 °C. 50 g of cenospheres was mixed into 100 mL of this solution.

Further, 2 % by volume of APTS was added into the solution and continuously stirred for 30 min at 80 °C in a microwave reactor (Enerzi Microwave Systems). Finally, the resultant product was filtered and washed at least three times using a mix of water/ethanol and then dried in an oven to extract the coated cenospheres. The cenospheres were analyzed by Fourier transform infrared (FTIR) spectroscopy to confirm the silane coating.

*HDPE functionalization*

In order to obtain strong bonding of HDPE with the silane coating layer of cenospheres, the HDPE was mixed with DBM. 0.15 g of dicumyl peroxide is added to 50 g of HDPE and 5 ml of DBM. The blend was mixed in the Brabender (CMEI, MODEL-16 CME SPL, Western Company Keltron) at 165 °C for 10 min.

**Sample preparation**

Cenospheres are first mixed with the HDPE resin using either mechanical or Brabender mixing methods. This mixture is fed into an industrial-scale horizontal-type single screw injection molding (IM) machine (WINDSOR, 80 ton capacity) to mold the flexural test specimens. The specimens are of dimensions  $127 \times 12.7 \times 3.2 \text{ mm}^3$ , which conforms to the ASTM D790-10 standard. The operating parameters of the IM machine for molding cenosphere/HDPE syntactic foams specimens were optimized in an earlier study [45] and were set at temperature of 160 °C and pressure of 30 kg/cm<sup>2</sup>. The three types of syntactic foams fabricated in the present study are listed in Table 2. Three compositions of syntactic foams containing

**Table 1** Chemical, physical, and sieve analysis details of cenospheres

Physical properties		Chemical analysis		Sieve analysis	
True particle density	800 kg/m <sup>3</sup>	SiO <sub>2</sub>	52–62 %	+ 30 # (500 μm)	Nil
Bulk density	400–450 kg/m <sup>3</sup>	Al <sub>2</sub> O <sub>3</sub>	32–36 %	+ 60 # (250 μm)	Nil
Hardness (MOH)	5–6	CaO	0.1–0.5 %	+100 # (150 μm)	Nil
Compressive strength	180–280 kg/m <sup>3</sup>	Fe <sub>2</sub> O <sub>3</sub>	1–3 %	+120 # (125 μm)	Nil
Shape	Spherical	TiO <sub>2</sub>	0.8–1.3 %	+150 # (106 μm)	0–10 %
Packing factor	60–65 %	MgO	1–2.5 %	+ 240 # (63 μm)	70–95 %
Wall thickness	5–10 % of shell dia.	Na <sub>2</sub> O	0.2–0.6 %	–240 #	0–30 %
Color	Light gray–light buff	K <sub>2</sub> O	1.2–3.2 %		
Melting point	1200–1300 °C	CO <sub>2</sub>	70 %		
pH in water	6–7	N <sub>2</sub>	30 %		
Moisture	0.5 % max.				
Loss on ignition	2 % max.				
Sinkers	5 % max.				
Oil absorption	16–18 g/100 g				

As specified by supplier

**Table 2** Syntactic foam types fabricated in the present study

Specimen Type	Cenospheres	HDPE	Mixing method
T <sub>M</sub> -MM	Untreated	Functionalized	Mechanical mixing
T-MM	Silane treated	Functionalized	Mechanical mixing
T-BM	Silane treated	Functionalized	Brabender mixing

cenospheres in 20, 40, and 60 wt% quantities are fabricated under each of the three conditions listed in Table 2. The corresponding specimen nomenclature is presented in Table 3. A block diagram detailing the specimen preparation procedure is presented in Fig. 1. For comparison, neat functionalized HDPE samples are also cast under the same processing conditions. The mixing in Brabender is carried out at 210 °C [17].

### Flexural testing

The flexural testing is performed in three-point bend configuration using a computer-controlled Zwick (Zwick Roell Z020, ZHU) machine having a load cell capacity of 20 kN. ASTM D790-10 is adopted for testing. A pre-load of 0.1 MPa is set, and crosshead displacement rate is maintained at 1.54 mm/min. All specimens have span length of

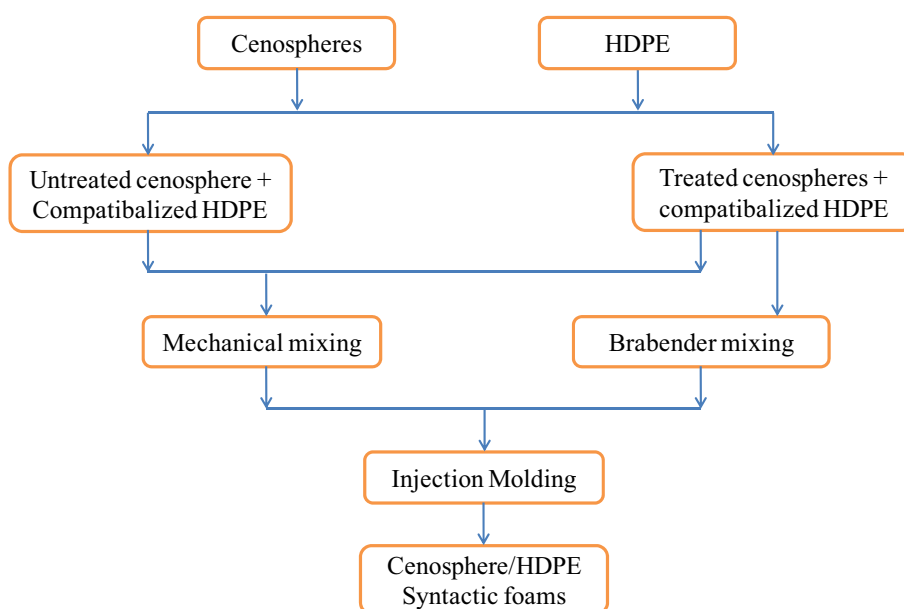
52 mm to maintain 16:1 span length/thickness ratio. Five specimens are tested, and the average values of the measured properties are presented. Tests are continued until 10 % strain to check the possibility of specimen failure, and the stress–strain data are acquired. The specimens did not show complete fracture in any syntactic foam at this strain level; therefore, results are reported in figures only up to 5 % strain for clarity. The flexural modulus ( $E$ ) is calculated by

$$E = \frac{L^3 m}{4bd^3}, \quad (1)$$

where  $L$  is the support span (mm),  $b$  is the width of beam (mm),  $d$  is the thickness of beam (mm), and  $m$  is the slope of the tangent to the initial straight-line portion of the load–deflection curve. The flexural stress ( $\sigma_{FM}$ ) is estimated by

**Table 3** Syntactic foam nomenclature scheme

Nomenclature	Remarks
HXX-Y-ZZ	Syntactic foam type
H	HDPE (neat matrix)
XX	Cenosphere by wt%
Y	Surface treated constituents ( $T$ ), HDPE functionalized ( $T_M$ )
ZZ	Mixing of constituents (mechanically mixed—MM, Brabender mixed—BM)

**Fig. 1** Processing routes and the types of cenosphere/HDPE syntactic foams synthesized in the present work

$$\sigma_{fM} = \frac{3PL}{2bd^2}, \quad (2)$$

where  $P$  is the load at a given point on the load–deflection curve ( $N$ ). The reported flexural strength values are taken at 5 % strain for comparison.

## Imaging

Scanning electron microscopes JSM 6380LA (JEOL, Japan) and S-3400N (Hitachi America Ltd., Tarrytown, NY) are used for conducting microstructure analysis. All the samples are sputter coated with gold using a JFC-1600 auto fine coater (JEOL, Japan).

## Results and discussion

### Material processing

A representative freeze-fractured specimen processed with a blend of as-received HDPE and 60 wt% cenospheres without any surface treatment is shown in Fig. 2a. Fly ash cenospheres are embedded in the resin but the resin flows around them without any interface formation. This can be observed more clearly in the micrograph at higher magnification (Fig. 2b), wherein the cenospheres are debonded from the HDPE matrix indicating lack of adhesion. While compressive properties are relatively less sensitive to poor interfacial bonding, tensile and flexural properties strongly depend on the interfacial bonding characteristics to transfer load from the matrix to the particle. Therefore, improvement in the cenosphere–HDPE interfacial bonding is highly desired. In order to achieve the strong interfacial bonding, cenospheres are treated with silane, and HDPE is functionalized with DBM.

Figure 3 presents FTIR spectra of non-functionalized and functionalized HDPE. DBM is added in dissolved solution of HDPE in proportions of 5, 10, and 15 % by

volume to check the variations in transmittance in FTIR (Fig. 3b). As observed from the figure, the variation in the spectra of specimens containing 5 and 10 vol.% DBM is negligible. HDPE functionalized with 10 vol.% DBM was chosen for use in the present work based on the previous published literature, which suggested that the modulus of the resin is reduced due to functionalization [17]. Figure 4 presents freeze-fractured micrographs of virgin and functionalized HDPE. High degree of surface roughness is observed in the fractured virgin specimen (Fig. 4a), whereas a few large cracks are observed in the functionalized specimen surface (Fig. 4b). Since total energy absorption in fracture depends on the area of the fracture surface, it is expected that the functionalized and non-functionalized specimens would show different mechanical properties when the quantitative results are compared.

FTIR results for untreated and silane-treated cenospheres are presented in Fig. 5. The spectrum confirms the presence of a silane surface layer, and the  $-C-H-$  stretching of propyl group is observed at  $2929\text{ cm}^{-1}$ . Micrographs of uncoated and silane-coated cenospheres are shown in Fig. 6a, b, respectively. The coating layer is not visibly identifiable in the micrographs due to its small thickness, despite the FTIR results providing evidence for its presence. Further observations are presented in Fig. 7a, b for broken untreated and silane-treated cenospheres, respectively. It is observed in both figures that the wall thickness of cenospheres is irregular, and there is significant amount of porosity in cenosphere walls. The porosity leads to lower strength of cenospheres than that expected from the fully dense walls of the same thickness. The results of particle size analysis for untreated and silane-treated cenospheres are presented in Fig. 8. It can be observed that the volume-weighted mean particle size for untreated particles is  $99.5\ \mu\text{m}$ . The peak for the coated particles is broader and shows the average value of  $110.2\ \mu\text{m}$ . The  $x_{50}$  median particle sizes are 76.3 and  $98.1\ \mu\text{m}$  for the treated and untreated particles. The

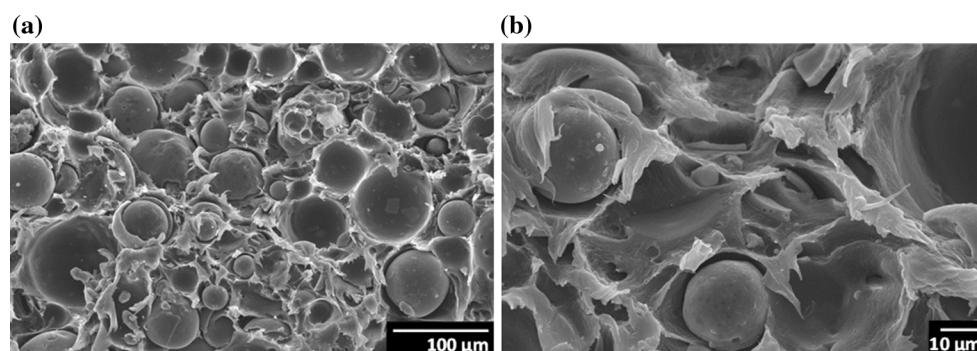


**Fig. 2** Microstructure of a representative specimen of syntactic foam fabricated with as-received cenospheres and HDPE. No bonding between particles and matrix is observed in these images

**Fig. 3** FTIR Spectra of **a** neat HDPE and **b** HDPE functionalized with 5, 10, and 15 % DBM. Note that the y-scales are different in both figures

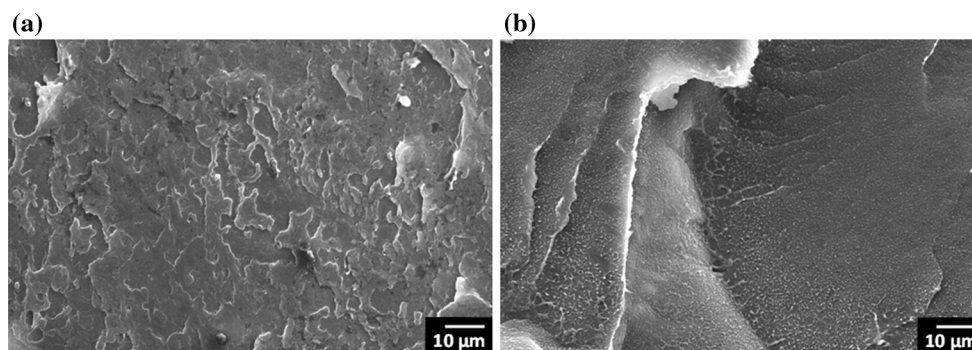
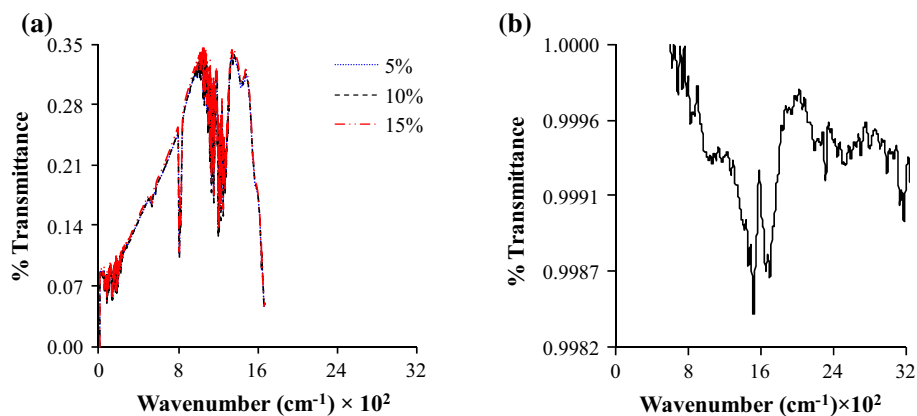


**Fig. 4** Freeze-fractured micrographs of **a** non-functionalized and **b** functionalized HDPE specimens at the same acquisition magnification

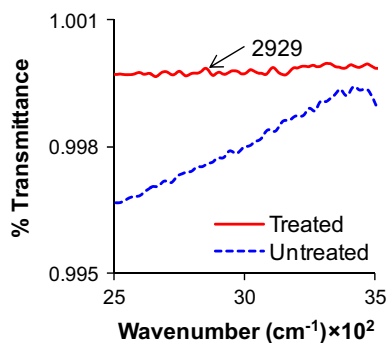
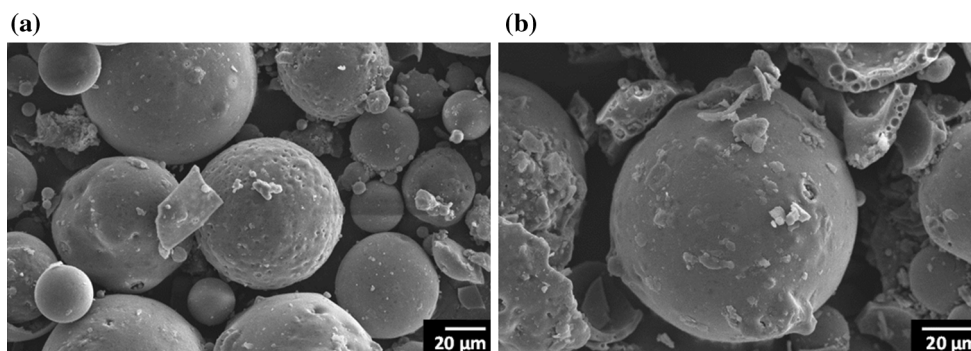


**Fig. 5** A section of the FTIR Spectra of untreated and silane-coated cenospheres

**Fig. 6** Micrographs of **a** untreated and **b** silane-treated cenospheres



increase in the average diameter can be partly attributed to the silane coating. It is also noted that some of small size particles sink during the surface treatment due to their high density and are not recovered back, which also contributes to the increased overall size of the coated particles. A shift in the initial part of the graph in Fig. 8 provides evidence for this possibility. It can be observed in Fig. 8 that the size distribution of uncoated particles is very narrow, and the upper range of particle size is about 170  $\mu\text{m}$ . In comparison, the tail end of the curve for the coated particle extends considerably to a maximum size of about 475  $\mu\text{m}$ . The probability density distribution for the larger size particles is very low. This observation indicates the formation of a

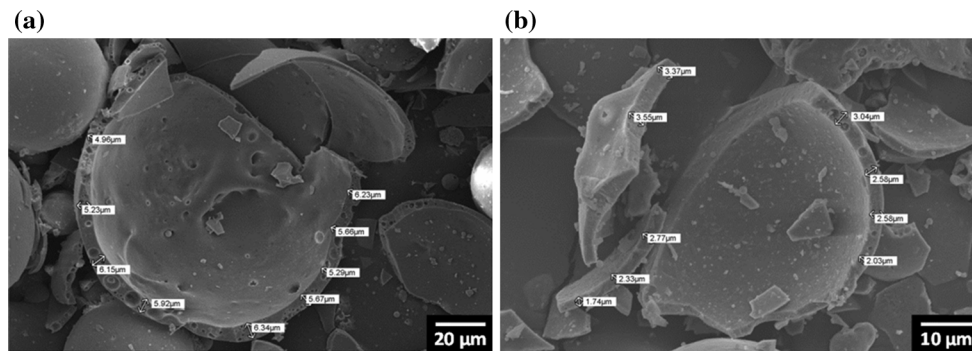


**Fig. 7** Micrographs of broken **a** untreated and **b** silane-treated cenospheres. The wall thickness variations within one particle and porosity that exists in the walls of these cenospheres can be observed in these micrographs

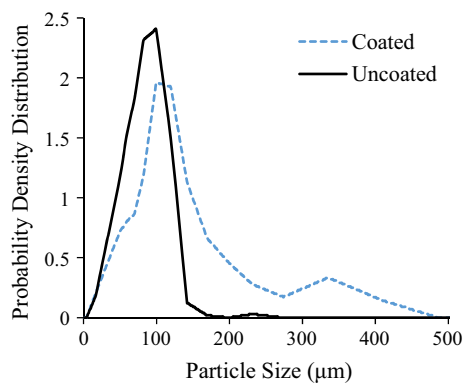


**Fig. 8** Particle size analysis of uncoated and silane-treated cenospheres

small amount of clusters as a result of silane treatment. It is expected that the shear forces applied during pre-mixing and injection molding will help in dispersing some of these clusters.

A typical microstructure of syntactic foams synthesized in the present work is presented in Fig. 9a. This figure shows that cenospheres are uniformly dispersed in functionalized HDPE resin. A higher magnification micrograph in Fig. 9b shows that the bonding between silane-treated cenospheres and the functionalized matrix is good. No separation or discontinuity is observed at the particle–matrix interface. Strong interfacial bonding is desired in applications where these composites can be subjected to tensile or flexural loading to enable effective transfer of load between particle and matrix. The ester-functionalized HDPE interacts with the amine group of silanized cenospheres, thereby, anchoring both HDPE and filler particles.

### Density and particle breakage during synthesis

The difference between experimental and theoretical (calculated using rule of mixtures) densities is presented for all syntactic foams in Table 4. Since no porosity is present in

HDPE matrix, the difference between theoretical and experimental density values is attributed to the cenosphere breakage during manufacturing and is estimated by

$$V_{mp} = \frac{\rho_t - \rho_m}{\rho_t}, \quad (3)$$

where  $V_{mp}$ ,  $\rho_t$ , and  $\rho_m$  are cenosphere porosity and theoretical and measured densities of syntactic foams. Negative porosity values indicate cenosphere breakage. During the syntactic foam synthesis using pressurized techniques like PIM, some cenospheres fracture. The matrix resin fills the cavity exposed due to cenosphere fracture, increasing the density of the syntactic foam. Some of the previous studies have shown measured density of syntactic foams to be higher than their theoretical densities despite the presence of matrix porosity, which leads to a conclusion that there was excessive fracture of hollow particles in those foams during synthesis [46]. In the present case, experimental density is higher than the theoretical density values, implying particle breakage. The particle fracture is low in composites containing 20 wt% cenosphere. However, as the cenosphere content is increased in the syntactic foam, the proportion of cenosphere breakage also increases, likely because of particle-to-particle interaction. In syntactic foams containing 60 wt% cenospheres, 18–25 wt% cenospheres are found to break due to the rigorous mixing procedure adopted. The results for both mechanical and Brabender mixing procedures are nearly the same. Higher particle breakage shows that the selected method can be used for manufacturing syntactic foams having up to 40 wt% cenospheres [45]. Higher quality specimens having lower fraction of particle breakage can be manufactured by other methods as has been demonstrated under laboratory conditions with greater control over environment. However, use of an industrial-scale machine allows evaluating the actual material quality that can be delivered if a product is developed. The specimens containing 60 wt% cenospheres will be evaluated to understand if broken particles provide any benefit in the material properties.

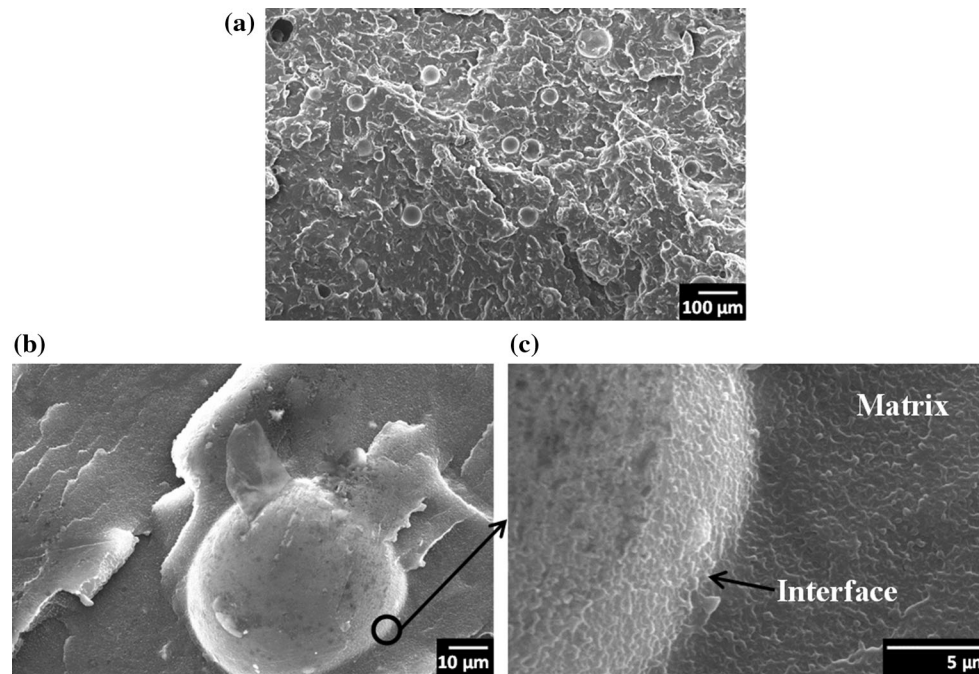


**Fig. 9** a Freeze-fractured micrographs of H60-T-BM syntactic foam showing dispersion of cenospheres in HDPE resin and **b** the interface between functionalized HDPE matrix and silane-treated cenospheres.

**c** The region marked by a circle in **(b)** is shown at higher magnification, where continuity across the interface can be observed. These micrographs are taken prior to the flexure test

**Table 4** Estimate of cenosphere failure during flexural test specimen synthesis (wt%)

Syntactic foam type	Theoretical density ( $\text{g/cm}^3$ )	Experimental density ( $\text{g/cm}^3$ )	Cenosphere failure (wt%)
H20-T <sub>M</sub> -MM	0.9976	$1.0326 \pm 0.0316$	3.51
H40-T <sub>M</sub> -MM	0.9430	$1.0293 \pm 0.0414$	9.15
H60-T <sub>M</sub> -MM	0.8923	$1.0548 \pm 0.0527$	18.21
H20-T-MM	0.9976	$1.083 \pm 0.0349$	8.56
H40-T-MM	0.9430	$1.111 \pm 0.0455$	17.82
H60-T-MM	0.8923	$1.114 \pm 0.0657$	24.85
H20-T-BM	0.9976	$1.049 \pm 0.0394$	5.15
H40-T-BM	0.9430	$1.071 \pm 0.0434$	13.57
H60-T-BM	0.8923	$1.074 \pm 0.0537$	20.36

### Flexural behavior

A representative stress–strain curve obtained from the flexural testing for functionalized HDPE resin is presented in Fig. 10a. The HDPE resin shows a non-linear behavior in this graph. The specimen did not fail even after 10 % strain, and therefore, the test was stopped. There was no visible sign of fracture during testing. The stress–strain behaviors of syntactic foam specimens prepared by different blending routes are presented in Fig. 10b–d. The trend of the stress–strain curves is similar for all composite types. Only a small initial portion is linear elastic, while the most part of these curves is non-linear elastic and plastic. It can be observed from this figure that the strength of

syntactic foam increases with the cenosphere content. This trend is very weak in the case of T-MM specimens (Fig. 10c). This combination of materials and processing method resulted in the lowest survival rate of cenospheres. Figure 11 presents a comparison of stress–strain graphs with respect to different blending methods. Syntactic foams processed by Brabender mixing show the highest level of strength, especially when the particle content is high. These results show the effectiveness of Brabender in dispersing cenospheres in the resin. Improved dispersion results in increased cenosphere–matrix interfacial bonding area and enhances the mechanical properties of syntactic foams. Table 4 shows that the cenosphere fracture is lower in Brabender mixed material compared to mechanically



**Fig. 10** Stress–strain behavior of **a** functionalized neat HDPE, and H20, H40, and H60 prepared by **b** T<sub>M</sub>-MM, **c** T-MM, and **d** T-BM routes

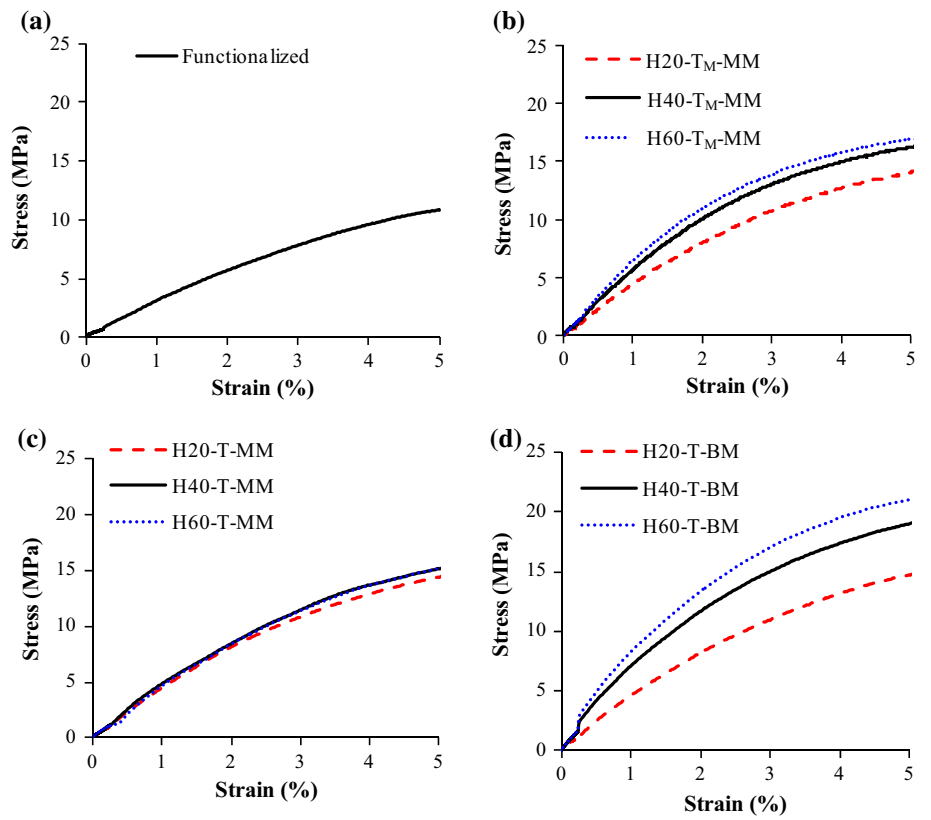
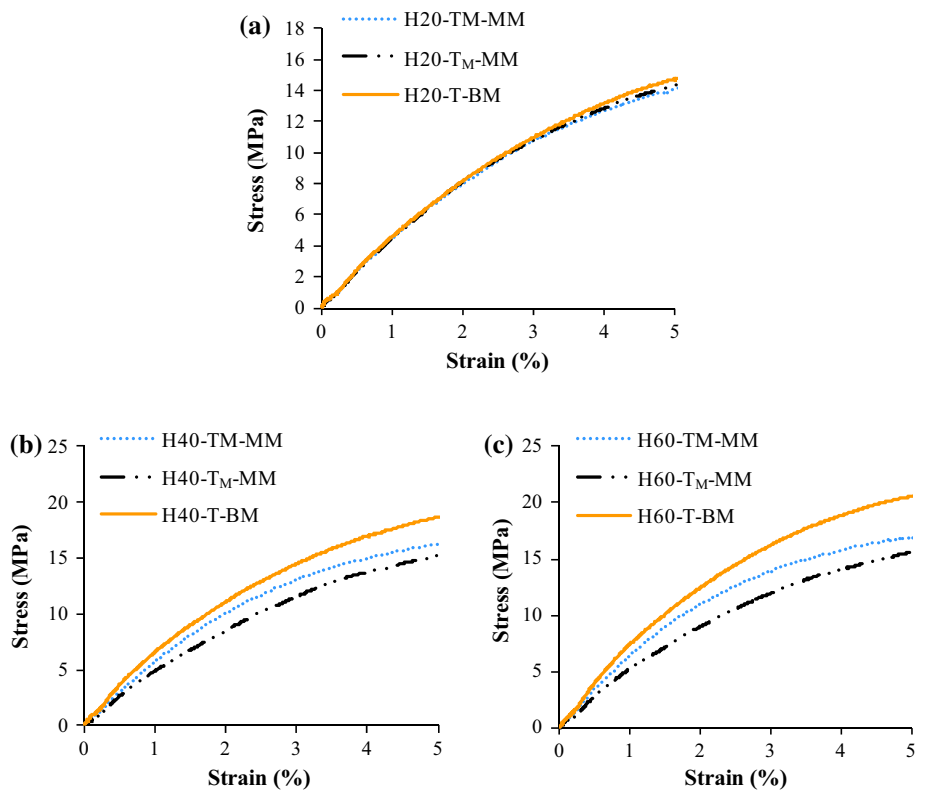


**Fig. 11** Comparison of stress–strain response for **a** H20 **b** H40 and **c** H60 syntactic foams as a function of blending methodology



mixed material. Reduced particle breakage is also likely to contribute to increased strength because the uncoated interior surfaces of the broken hollow particles are unable to bond with the matrix. The more rigorous mixing in Brabender blending may also help in improving the interface with these untreated surfaces.

Flexural modulus values for all syntactic foams are presented in Fig. 12a. The modulus is found to increase with cenosphere content. Higher stiffness of cenosphere material compared to the HDPE resin helps in obtaining improvement in the stiffness of syntactic foams as the cenosphere content is increased. Compared to the modulus of functionalized HDPE, 204.7 MPa, the H60-T<sub>M</sub>-MM, H60-T-MM, and H60-T-BM syntactic foams had 70, 51, and 69 % higher modulus. The flexural strengths for syntactic foams are presented in Fig. 12b. The flexural strength is also found to increase with cenosphere content. All syntactic foams have higher strength than that of the HDPE resin. Compared to the strength of functionalized HDPE, 12.4 MPa, the H60-T<sub>M</sub>-MM, H60-T-MM, and H60-T-BM syntactic foams had 31, 27, and 41 % higher strength. Brabender mixing of silane-treated particles and functionalized HDPE resin provides the highest benefit in flexural strength.

### Theoretical analysis

The bending behavior of the syntactic foams is analyzed using two theoretical models. Porfiri–Gupta model has been validated for epoxy and vinyl ester matrix syntactic foams containing engineered glass hollow particles [47–49]. This model employs a differential scheme to solve for the elastic properties of an infinitely dilute dispersion of particles in a matrix and then extends the solution to high particle loadings. The differential scheme, with a correction factor to account for the reduced volume available for particles to occupy as the particle loading increases, is given as

$$\frac{dE}{E} = f_E(E_c, \nu_c, E_m, \nu_m, \eta) \frac{d\Phi}{1 - \Phi/\Phi_{\max}}, \quad (4)$$

where  $E$  and  $\nu$  are the Young's modulus and Poisson's ratio, and the subscripts  $c$  and  $m$  refer to the ceramic particle wall and the matrix resin, respectively. In addition,  $\Phi$  represents cenospheres volume fraction and  $\Phi_{\max}$  denotes the maximum packing factor of particles in syntactic foam, taken to be 0.637, which represents the random packing factor of equal size spheres.

Bardella–Genna model [50, 51] considers a representative volume element and uses a homogenization scheme to estimate the bulk and shear moduli of the composite. The bulk modulus of the composite is given as

$$K = K_m \frac{\delta(1 + \Phi\gamma) + \kappa(1 - \Phi)\gamma}{\delta(1 - \Phi) + \kappa(\gamma + \Phi)}, \quad (5)$$

where

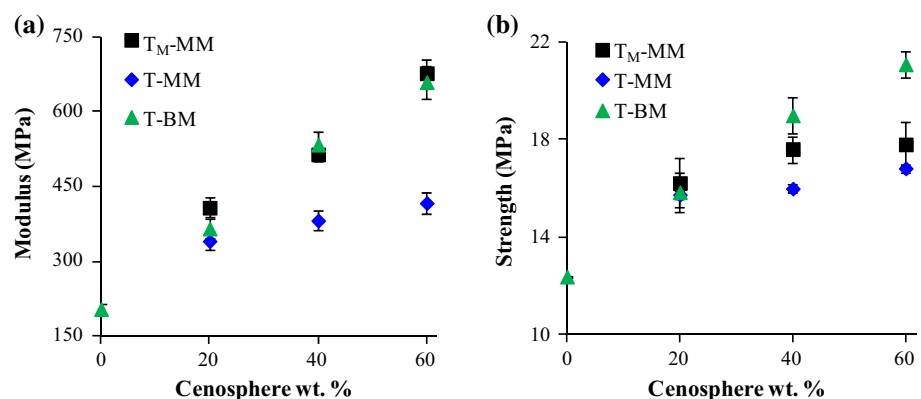
$$\gamma = \frac{4G_m}{3K_m} \quad \delta = \frac{4G_c}{3K_m}(1 - \eta^3) \quad \kappa = \frac{4G_c}{3K_c} + \eta^3 \quad (6)$$

The  $G$  and  $K$  terms represent the shear and bulk moduli of the materials, which are derived from the elastic modulus and Poisson's ratio for each material. The parameter  $\eta$  in the models is the radius ratio of the hollow particles, defined as the ratio of the inner radius to the outer radius of the sphere. Detailed expressions for shear modulus calculations can be found in the original work [50, 51]. These two elastic constants then allow for the determination of the elastic modulus of syntactic foams by

$$E = \frac{9KG}{3K + G}. \quad (7)$$

The modulus of the matrix is taken from the experimental data, and the Poisson's ratio is taken to be 0.425 [52]. The properties of the cenosphere wall are determined according to the rule of mixtures approach presented by [53], where the properties of the constituent materials of the particle wall are used to estimate the properties of the

**Fig. 12** **a** Flexural modulus and **b** flexural strength of syntactic foams at different cenosphere contents



wall material. The two major constituent materials, namely SiO<sub>2</sub> and Al<sub>2</sub>O<sub>3</sub>, are accounted for, while minor constituents are ignored, which leads to estimates for the modulus and Poisson’s ratio of 158 GPa and 0.185, respectively. The value of  $\eta$  for cenospheres is estimated using the assumption of uniform fully dense walls using [54]

$$\eta = \sqrt[3]{1 - \frac{\rho_{TPD}}{\rho_c}} \tag{8}$$

where  $\rho_{TPD}$  is the true particle density and  $\rho_c$  is the density of the ceramic, also obtained by the rule of mixtures for cenosphere considering alumino-silicate composition. Using this method, the radius ratio is determined to be 0.903 for the cenospheres used in this work. This method yields similar results to the particle wall thickness measurements shown in Fig. 7, which give an average radius ratio of 0.897 for the particle in Fig. 7a.

The predictions of the two models are compared to the experimental data in Fig. 13. The volume fractions of cenospheres are reduced by the calculated fraction of broken particles. The two models are in close agreement for a dilute dispersion of particles, or up to 20 vol.%, but diverge at higher particle loadings due to increased particle-to-particle interactions and lower matrix content. At higher volume fractions, the Porfiri–Gupta model diverges, while the Bardella–Genna model shows closer agreement with the experimental data for T<sub>M</sub>-MM and T-BM syntactic foams. The Bardella–Genna model can be used for identifying the parameters such as cenosphere volume fraction and true particle density that are expected to provide syntactic foams of desired properties. It is noted that the experimental values of modulus are lower than the predictions for 40 and 60 wt% particles. This kind of trend is likely due to the presence of broken particles as stress concentration sites due to thin walls of cenospheres.

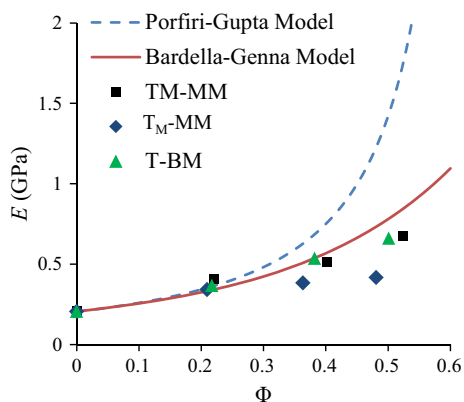


**Fig. 13** Comparison of model predictions with experimental data on modulus of syntactic foams

### Conclusions

A comprehensive study is conducted to investigate the effect of surface treatment and blending method on flexural response of cenosphere/HDPE syntactic foams fabricated through injection molding technique. Optimized processing parameters for the polymer injection molding process are used from an earlier work. Use of cenospheres in consumer products can make them lighter, reduce the consumption of HDPE, and address the environmental concern of fly ash disposal. Syntactic foams with 20, 40, and 60 wt% are fabricated. The main conclusions can be summarized as follows:

- Microscopic observations reveal poor interfacial bonding between the as-received cenospheres and HDPE. The surface treatment of cenospheres and functionalization of HDPE promote interfacial bonding.
- The breakage of cenospheres increases with their weight fraction due to increased particle-to-particle interaction during mixing in the present industrial-scale manufacturing method.
- Flexural modulus and strength are found to increase with cenosphere content for syntactic foams manufactured by all methods.
- The modulus and strength are found to be the highest for specimens blended by Brabender mixing before injection molding.
- The functionalized HDPE was measured to have flexural modulus and strength of 205 and 12.4 MPa, respectively. In comparison, the 60 wt% cenosphere containing syntactic foams processed through Brabender mixing resulted in the highest flexural modulus and strength of 660 and 21 MPa, respectively. These values are 70 and 41 % higher than the corresponding values for the HDPE resin.
- Two theoretical models are used for prediction of modulus of the syntactic foams. Bardella–Genna model predictions are close to the experimental results. This model can be used for designing syntactic foam microstructures with desired properties.

It is desired to reduce the particle breakage in higher loading compositions. However, syntactic foams containing up to 40 wt% particles can be fabricated with these processes with good quality.

**Acknowledgements** The authors acknowledge Dr. Keshav Prabhu, Mr. Puneeth, and Mr. Praveen of Konkan Speciality Polyproducts Pvt. Ltd., Mangalore, Karnataka, India for providing the Injection molding facility for casting the samples and useful discussions. Acknowledgement is also due to Director, TERI, for providing Brabender facility for preparing the blends. Author Nikhil Gupta acknowledges the Office of Naval Research Grant N00014-10-1-0988. The views expressed in this article are those of authors, not of funding agencies.

The authors thank the ME Department at NIT-K and MAE Department at NYU for providing facilities and support.

## References

- Gupta N, Zeltmann S, Shunmugasamy V, Pinisetty D (2013) Applications of Polymer Matrix Syntactic Foams. *JOM*, p 1–10
- Gupta N, Pinisetty D, Shunmugasamy VC (2013) Reinforced polymer matrix syntactic foams: effect of nano and micro-scale reinforcement. Springer International Publishing, Cham
- Yalcin B (2015) Chapter 7—hollow glass microspheres in polyurethanes. In: Amos SE, Yalcin B (eds) *Hollow glass microspheres for plastics, elastomers, and adhesives compounds*. William Andrew Publishing, Oxford, pp 175–200
- Yalcin B, Amos SE (2015) Chapter 3—hollow glass microspheres in thermoplastics. In: Amos SE, Yalcin B (eds) *Hollow glass microspheres for plastics, elastomers, and adhesives compounds*. William Andrew Publishing, Oxford, pp 35–105
- Bachmatiuk A, Börrnert F, Schäffel F, Zaka M, Martynkova GS, Placha D, Schönfelder R, Costa PMFJ, Ioannides N, Warner JH, Klingeler R, Büchner B, Rümmelel MH (2010) The formation of stacked-cup carbon nanotubes using chemical vapor deposition from ethanol over silica. *Carbon* 48(11):3175–3181
- Alkan C, Arslan M, Cici M, Kaya M, Aksoy M (1995) A study on the production of a new material from fly ash and polyethylene. *Resour Conserv Recycl* 13(3–4):147–154
- Li J, Agarwal A, Iveson SM, Kiani A, Dickinson J, Zhou J, Galvin KP (2014) Recovery and concentration of buoyant cenospheres using an Inverted Reflux Classifier. *Fuel Process Technol* 123:127–139
- Lauf RJ (1981) Cenospheres in fly ash and conditions favouring their formation. *Fuel* 60(12):1177–1179
- Anshits NN, Mikhailova OA, Salanov AN, Anshits AG (2010) Chemical composition and structure of the shell of fly ash non-perforated cenospheres produced from the combustion of the Kuznetsk coal (Russia). *Fuel* 89(8):1849–1862
- Gupta N, Singh Brar B, Woldesenbet E (2001) Effect of filler addition on the compressive and impact properties of glass fibre reinforced epoxy. *Bull Mater Sci* 24(2):219–223
- Satapathy B, Das A, Patnaik A (2011) Ductile-to-brittle transition in cenosphere-filled polypropylene composites. *J Mater Sci* 46(6):1963–1974. doi:10.1007/s10853-010-5032-0
- Qiao J, Wu G (2011) Tensile properties of fly ash/polyurea composites. *J Mater Sci* 46(11):3935–3941. doi:10.1007/s10853-011-5318-x
- Manakari V, Parande G, Doddamani M, Gaitonde VN, Sidhalingeshwar IG, Kishore, Shunmugasamy VC, Gupta N (2015) Dry sliding wear of epoxy/cenosphere syntactic foams. *Tribol Int* 92:425–438
- Labella M, Zeltmann SE, Shunmugasamy VC, Gupta N, Rohatgi PK (2014) Mechanical and thermal properties of fly ash/vinyl ester syntactic foams. *Fuel* 121:240–249
- Hossain MM, Shivakumar K (2011) Compression fatigue performance of a fire resistant syntactic foam. *Compos Struct* 94(1):290–298
- Doddamani M, Kishore, Shunmugasamy VC, Gupta N, Vijayakumar HB (2015) Compressive and flexural properties of functionally graded fly ash cenosphere–epoxy resin syntactic foams. *Polym Compos* 36(4):685–693
- Deepthi MV, Sharma M, Sailaja RRN, Anantha P, Sampathkumar P, Seetharamu S (2010) Mechanical and thermal characteristics of high density polyethylene–fly ash Cenospheres composites. *Mater Des* 31(4):2051–2060
- Wang W, Li Q, Wang B, Xu X-T, Zhai J-P (2012) Synthesis of fly ash cenosphere/polyaniline and mullite/polyaniline core–shell composites. *Mater Chem Phys* 135(2–3):1077–1083
- Guhanathan S, Devi MS, Murugesan V (2001) Effect of coupling agents on the mechanical properties of fly ash/polyester particulate composites. *J Appl Polym Sci* 82(7):1755–1760
- Chand N, Sharma P, Fahim M (2010) Correlation of mechanical and tribological properties of organosilane modified cenosphere filled high density polyethylene. *Mater Sci Eng A* 527(21–22):5873–5878
- Sharma J, Chand N, Bapat MN (2012) Effect of cenosphere on dielectric properties of low density polyethylene. *Results Phys* 2:26–33
- Patankar SN, Das A, Kranov YA (2009) Interface engineering via compatibilization in HDPE composite reinforced with sodium borosilicate hollow glass microspheres. *Compos A* 40(6–7):897–903
- Patankar SN, Kranov YA (2010) Hollow glass microsphere HDPE composites for low energy sustainability. *Mater Sci Eng A* 527(6):1361–1366
- Sailaja RRN (2006) Mechanical and thermal properties of bleached kraft pulp–LDPE composites: effect of epoxy functionalized compatibilizer. *Compos Sci Technol* 66(13):2039–2048
- Sailaja RRN, Seetharamu S (2008) Itaconic acid–grafted–LDPE as compatibilizer for LDPE–plasticized Tapioca starch blends. *React Funct Polym* 68(4):831–841
- Sailaja RRN, Deepthi MV (2010) Mechanical and thermal properties of compatibilized composites of polyethylene and esterified lignin. *Mater Des* 31(9):4369–4379
- Deepthi MV, Sailaja RRN, Sampathkumar P, Seetharamu S, Vynatheya S (2014) High density polyethylene and silane treated silicon nitride nanocomposites using high-density polyethylene functionalized with maleate ester: mechanical, tribological and thermal properties. *Mater Des* 56:685–695
- Chiu F-C, Yen H-Z, Lee C-E (2010) Characterization of PP/HDPE blend-based nanocomposites using different maleated polyolefins as compatibilizers. *Polym Testing* 29(3):397–406
- Parthasarathi V, Sundaresan B, Dhanalakshmi V, Anbarasan R (2010) Functionalization of HDPE with aminoester and hydroxyester by thermolysis method—an FTIR-RI approach. *Thermochim Acta* 510(1–2):61–67
- Gu J, Wu G, Zhao X (2009) Effect of surface-modification on the dynamic behaviors of fly ash cenospheres filled epoxy composites. *Polym Compos* 30(2):232–238
- Huo P, Yan Y, Li S, Li H, Huang W, Chen S, Zhang X (2010) H<sub>2</sub>O<sub>2</sub> modified surface of TiO<sub>2</sub>/fly-ash cenospheres and enhanced photocatalytic activity on methylene blue. *Desalination* 263(1–3):258–263
- Desai J, Shit SC, Jain SK (2014) Studies on thermal, electrical and flame properties of surface modified cenosphere filled ABS composites. *Int J Plast Technol* 18(3):390–396
- Das A, Satapathy BK (2011) Structural, thermal, mechanical and dynamic mechanical properties of cenosphere filled polypropylene composites. *Mater Des* 32(3):1477–1484
- Maharsia R, Gupta N, Jerro HD (2006) Investigation of flexural strength properties of rubber and nanoclay reinforced hybrid syntactic foams. *Mater Sci Eng A* 417(1–2):249–258
- Tagliavia G, Porfiri M, Gupta N (2010) Analysis of flexural properties of hollow-particle filled composites. *Compos B Eng* 41(1):86–93
- Tagliavia G, Porfiri M, Gupta N (2012) Influence of moisture absorption on flexural properties of syntactic foams. *Compos B Eng* 43(2):115–123
- Lin W-H, Jen M-HR (1998) Manufacturing and Mechanical Properties of Glass Bubbles/Epoxy Particulate Composite. *J Compos Mater* 32(15):1356–1390

38. Kishore, Shankar R, Sankaran R (2005) Short beam three point bend tests in syntactic foams. Part I: microscopic characterization of the failure zones. *J Appl Polym Sci* 98(2):673–679
39. Kishore, Shankar R, Sankaran S (2005) Short-beam three-point bend tests in syntactic foams. Part II: effect of microballoons content on shear strength. *J Appl Polym Sci* 98(2):680–686
40. Kishore, Shankar R, Sankaran S (2005) Short-beam three-point bend test study in syntactic foam. Part III: effects of interface modification on strength and fractographic features. *J Appl Polym Sci* 98(2):687–693
41. Zhu B, Ma J, Wang J, Wu J, Peng D (2012) Thermal, dielectric and compressive properties of hollow glass microsphere filled epoxy-matrix composites. *J Reinf Plast Compos* 31(19):1311–1326
42. Yung KC, Zhu BL, Yue TM, Xie CS (2009) Preparation and properties of hollow glass microsphere-filled epoxy-matrix composites. *Composit Sci Technol* 69(2):260–264
43. Poveda RL, Dorogokupets G, Gupta N (2013) Carbon nanofiber reinforced syntactic foams: degradation mechanism for long term moisture exposure and residual compressive properties. *Polym Degrad Stab* 98(10):2041–2053
44. Divya VC, Ameen Khan M, Nageshwar Rao B, Sailaj RRN (2015) High density polyethylene/cenosphere composites reinforced with multi-walled carbon nanotubes: mechanical, thermal and fire retardancy studies. *Mater Des* 65:377–386
45. Bharath Kumar BR, Doddamani M, Zeltmann SE, Gupta N, Ramesh MR, Ramakrishna S (2016) Processing of cenosphere/HDPE syntactic foams using an industrial scale polymer injection molding machine. *Mater Des* 92:414–423. doi:[10.1016/j.matdes.2015.12.052](https://doi.org/10.1016/j.matdes.2015.12.052)
46. Huang JS, Gibson LJ (1991) Fracture toughness of brittle foams. *Acta Metall Mater* 39(7):1627–1636
47. Porfiri M, Gupta N (2009) Effect of volume fraction and wall thickness on the elastic properties of hollow particle filled composites. *Compos B* 40(2):166–173
48. Gupta N, Ye R, Porfiri M (2010) Comparison of tensile and compressive characteristics of vinyl ester/glass microballoon syntactic foams. *Compos B* 41(3):236–245
49. Aureli M, Porfiri M, Gupta N (2010) Effect of polydispersivity and porosity on the elastic properties of hollow particle filled composites. *Mech Mater* 42(7):726–739
50. Bardella L, Genna F (2001) On the elastic behavior of syntactic foams. *Int J Solids Struct* 38(40–41):7235–7260
51. Bardella L, Sfreddo A, Ventura C, Porfiri M, Gupta N (2012) A critical evaluation of micromechanical models for syntactic foams. *Mech Mater* 50:53–69
52. Gabriel LH (1998) History and physical chemistry of HDPE. Ohio University, Ohio
53. Matsunaga T, Kim JK, Hardcastle S, Rohatgi PK (2002) Crystallinity and selected properties of fly ash particles. *Mater Sci Eng A* 325(1–2):333–343
54. Shunmugasamy V, Zeltmann S, Gupta N, Strbik O III (2014) Compressive Characterization of Single Porous SiC Hollow Particles. *JOM* 66(6):892–897